JOURNAL OF MAGNETIC RESONANCE 99, 652–659 (1992)

Three-Dimensional NMR Experiments for the Separation of Side-Chain Correlations in Proteins via the Carbonyl Chemical Shift

LEWIS E. KAY,* MITSUHIKO IKURA,† A. A. GREY,‡ AND D. R. MUHANDIRAM*

*Departments of Medical Genetics, Biochemistry, and ‡Carbohydrate Research Center, and Chemistry, Medical Sciences Building, University of Toronto, Toronto, Ontario, Canada M5S 1A8; and †Ontario Cancer Institute and Department of Medical Biophysics, University of Toronto, 500 Sherbourne Street, Toronto, Ontario, Canada M4X 1K9

Received July 7, 1992

Assignment of side-chain resonances is an essential component of the determination of protein structures by NMR methods. For small proteins with molecular weights less than approximately 10 kDa, side-chain assignment is achieved through the use of homonuclear Hartmann–Hahn/TOCSY (*1, 2*) and COSY (*3*) spectroscopy. These techniques rely on magnetization transfer via ^1H–^1H scalar couplings. For proteins with molecular weights in excess of ~10 kDa, ^1H linewidths are often significantly larger than the ^1H–^1H scalar couplings, which greatly decreases the applicability of these methods. The recently introduced HCCH–COSY (*4*), CCH–TOCSY (*5*), and HCCH–TOCSY (*6*) experiments transfer magnetization via the large (35–40 Hz) one-bond ^{13}C–^{13}C couplings. The transfer efficiency of magnetization in these experiments is superior to that of the transfer in experiments relying on ^1H couplings since homonuclear ^{13}C–^{13}C couplings are much larger than the corresponding ^1H couplings. In addition, by extending the dimensionality of these experiments to three, the resolution is greatly improved and assignment of side-chain ^1H and ^{13}C resonances in proteins with molecular weights as large as 20 kDa is possible (*7, 8*).

Despite the tremendous improvements in sensitivity and resolution that the HCCH–COSY and HCCH–TOCSY experiments provide, overlap of resonances may still occur, especially for cross peaks originating from structurally similar residues. For example, despite the relatively small size of the protein *Drosophila* calmodulin (148 amino acids), the large number of aspartic acid and glutamic acid residues (16 aspartic acids and 20 glutamic acids) and the existence of four highly homologous structural motifs in the protein complicate the side-chain assignment for these residues. In this situation, it would be useful to separate COSY and TOCSY side-chain connectivities by an alternate chemical shift, such as the carbonyl shift. Then, in residues with degenerate Hα and Cα chemical shifts but nondegenerate carbonyl (C′) chemical shifts, it would be straightforward to assign side-chain resonances in data sets where side-chain connectivities were separated by carbonyl shifts. In addition, automated assignment procedures would be more applicable.

In this Communication we present a number of experiments for correlating side-chain resonances which use the carbonyl shift to separate correlations. The first two experiments, termed HCACO–COSY and HCACO–TOCSY, provide correlations be-

0022-2364/92 $5.00

tween Hα protons and protons on the same side chain. The third dimension in these experiments encodes the intraresidue carbonyl chemical shift. Briefly, magnetization originating on the Hα proton is transferred to the carbonyl spin via the intervening Cα spin in a manner identical to the transfer scheme of the HCACO experiment (*9*). The C′ chemical shift is recorded and magnetization returned to the Cα carbon. Subsequently magnetization is transferred along the side chain in either a COSY or TOCSY manner. Side-chain proton magnetization is detected during acquisition. The third experiment which we present, the HCACO–CBHB experiment, correlates C′, Cβ (Cα), and Hβ (Hα) chemical shifts and is closely related to the HCACO–COSY scheme.

The pulse sequences for the HCACO–TOCSY, HCACO–COSY, and HCACO–CBHB experiments are illustrated in Figs. 1a–1c, respectively. Since the magnetization-transfer steps in all of the pulse schemes are quite similar it suffices to consider an in-depth description of only one of the sequences. In what follows, a product-operator description of the HCACO–CBHB experiment is provided. For clarity, only those terms that contribute to observable magnetization are indicated, the effects of relaxation are neglected, constant multiplicative factors preceding the terms of interest are omitted, and the phases of all of the pulses are indicated in the first step of the phase cycle described in the legend to Fig. 1. The spin operators used are I and S for Hα and Cα spins, I′ and S′ for Hβ and Cβ spins, and C′ for the carbonyl spin. The effects of multiple-bond couplings are ignored and it is assumed that only a single Hα spin is attached to spin S.

The longitudinal magnetization at time a is described by an operator of the form $\rho_a = I_z$. Proton magnetization is allowed to evolve during $2\tau_a$ and is transferred in an INEPT-type manner (*10*) to the Cα spin. At time b, the relevant density operator is

$$\rho_b = I_z S_y \sin(2\pi J_{IS}\tau_a), \qquad [1]$$

where J_{IS} is the one-bond ^1H–^{13}C coupling. Magnetization on the Cα spin, which is antiphase with respect to the directly coupled Hα spin, is refocused during τ_b and subsequent evolution due to ^1H–^{13}C couplings eliminated by the application of WALTZ-16 decoupling (*11*) on the proton channel. The use of coherent decoupling schemes, such as WALTZ, to maintain in-phase carbon magnetization is preferable over schemes which refocus the effects of ^1H–^{13}C scalar couplings with 180° pulses since in macromolecules the relaxation time of the in-phase component of magnetization, $S_{(x,y)}$, is significantly longer than the relaxation time of the antiphase magnetization component, $S_{(x,y)}I_z$ (*12–14*). Cα magnetization dephases due to the Cα–C′ scalar coupling during the period $2\tau_b$ so that at time c, ρ_c is given by

$$\rho_c = S_y C'_z \sin(2\pi J_{SC'}\tau_b)\cos(2\pi J_{SS'}\tau_b), \qquad [2]$$

where $J_{SC'}$ and $J_{SS'}$ are the Cα–C′ and the Cα–Cβ scalar coupling constants, respectively, and it is assumed that $\tau_b = 1/(2J_{IS})$. Note that the factors associated with ρ_b have not been carried forward. Carbonyl and Cα pulses are adjusted so that the application of Cα pulses produces minimal effects in the carbonyl region of the spectrum and vice versa (*9*). Simultaneous application of 90° Cα and C′ pulses at time d yields

$$\rho_d = S_z C'_y. \qquad [3]$$

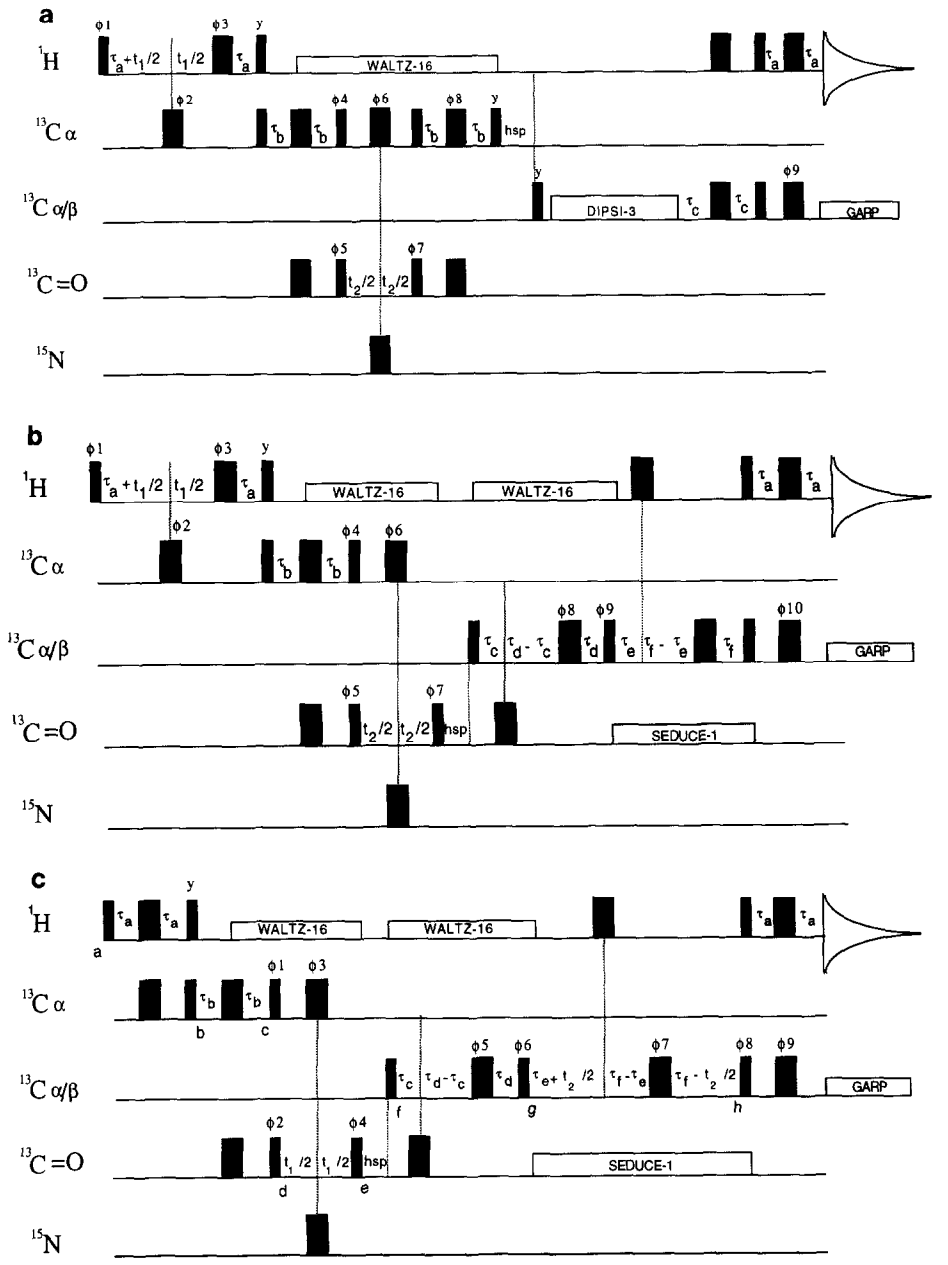

FIG. 1. (a) Pulse scheme of the HCACO-TOCSY experiment. All narrow pulses have a flip angle of 90° with wider pulses having a flip angle of 180°. Pulses for which the phases are not indicated are applied along the x axis. All Cα 90° pulses, prior to the homospoil pulse (hsp) and all C′ 90° and 180° pulses are adjusted to satisfy the condition that $\nu_1 = (\Delta\nu)/\sqrt{15}$, where $\Delta\nu$ is the offset between the centers of the Cα and the C′ regions of the carbon spectrum ($\sim$15.6 kHz for a 500 MHz spectrometer) and ν_1 is the RF field strength of the Cα or C′ pulse. In contrast, Cα 180° pulses are applied at a field strength satisfying the condition $\nu_1 = (\Delta\nu)/\sqrt{3}$. For these strengths of RF fields application of Cα pulses produces minimal effects in the carbonyl region of the carbon spectrum and vice versa. Carbon pulses applied prior to the hsp period are centered at 54 ppm, the middle of the Cα spectral region. For the application of successive carbon pulses it is advantageous to move the transmitter frequency midway between the Cα and Cβ regions of the spectrum. Since the

Carbonyl magnetization evolves for a period t_1 and the effects of ^{15}N–C′ and Cα–C′ couplings are refocused by the simultaneous application of ^{15}N and Cα 180° pulses in the center of the t_1 evolution period. Application of a 90° C′ pulse yields at time e an operator of the form

$$\rho_e = S_z C'_z \cos(\omega_{C'} t_1), \quad [4]$$

where $\omega_{C'}$ is the Larmor frequency of spin C′. All carbon pulses applied to this point have been centered at 54 ppm, the middle of the Cα spectral region. For the application of successive carbon pulses it is advantageous to move the transmitter frequency midway between the Cα and Cβ regions of the spectrum. In addition to jumping the carbon frequency, a homospoil pulse of duration 5–10 ms is applied to aid in the removal of magnetization originating from unwanted coherence-transfer pathways. At time f the density operator is given by

$$\rho_f = S_y C'_z. \quad [5]$$

Subsequently, Cα magnetization is transferred to the Cβ spin in a COSY-type manner so that at time g the density operator is given by

$$\rho_g = S_z S'_y \sin(2\pi J_{SC'} \tau_c) \sin(2\pi J_{SS'} \tau_d). \quad [6]$$

---

synthesizer used for the application of carbon pulses on our spectrometer does not maintain a constant phase during a frequency jump, ^{13}C magnetization is transferred to the z axis prior to changing the frequency. Subsequently all carbon pulses are centered at 43 ppm and applied with a field strength of 7.8 kHz. A DIPSI-3 mixing scheme (*17*) is employed, preceded by a 2 ms trim pulse. The delays used are τ_a = 1.8 ms, τ_b = 3.6 ms, $2\tau_c = 0.3/J_{CH}$ = 2.1 ms. Prior to low-power decoupling (2.3 kHz field), a high-power $90^\circ_x 90^\circ_{\phi 10}$ pulse pair is applied in a manner described previously (*18*). The phase cycle used is $\phi_1 = x$; $\phi_2 = 16(x)$, $16(-x)$; $\phi_3 = 2(x)$, $2(-x)$; $\phi_4 = 4(x)$, $4(-x)$; $\phi_5 = x, -x$; $\phi_6 = 8(x)$, $8(-x)$; ϕ_7, $= 2(x)$, $2(-x)$; $\phi_8 = 8(x)$, $8(-x)$; $\phi_9 = 4(x)$, $4(-x)$; $\phi_{10} = 4(x)$, $4(-x)$; Rec = x, $2(-x)$, x, $-x$, $2(x)$, $-x$. Quadrature in t_1 and t_2 is obtained using the States–TPPI method (*19*), incrementing the phases ϕ_1 and ϕ_5. (b) Pulse scheme of the HCACO–COSY experiment. Prior to low-power decoupling (2.3 kHz field), a high-power $90^\circ_x 90^\circ_{\phi 11}$ pulse pair is applied (*18*). The $^{13}C\alpha$ 90° pulses and the $^{13}C'$ 90° and 180° pulses are applied with a field strength $\nu_1 = (\Delta\nu)/\sqrt{15}$ while the $^{13}C\alpha$ 180° pulses are applied at a field strength $\nu_1 = (\Delta\nu)/\sqrt{3}$. $^{13}C\alpha$ pulses are applied with the carbon transmitter at 54 ppm while $^{13}C\alpha/\beta$ pulses are centered at 43 ppm. Carbonyl decoupling is applied using the shaped decoupling sequence, SEDUCE-1 (*20*). A 600 Hz SEDUCE-1 decoupling field is applied. The delays used are τ_a = 1.8 ms, τ_b = 3.6 ms, τ_c = 4.3 ms, τ_d = 4.8 ms, τ_e = 1.1 ms, and τ_f = 3.6 ms. The phase cycling used is as follows: $\phi_1 = x$; $\phi_2 = 16(x)$, $16(-x)$; $\phi_3 = 2(x)$, $2(-x)$; $\phi_4 = 4(x)$, $4(-x)$; $\phi_5 = x, -x$; $\phi_6 = 8(x)$, $8(-x)$; $\phi_7 = 2(x)$, $2(-x)$; $\phi_8 = 8(x)$, $8(-x)$; $\phi_9 = 16(x)$, $16(-x)$; $\phi_{10} = 4(x)$, $4(-x)$; $\phi_{11} = 4(x)$, $4(-x)$; Rec = x, $2(-x)$, x, $-x$, $2(x)$, $-x$. Quadrature in t_1 and t_2 is obtained using the States–TPPI method (*19*), incrementing the phases ϕ_1 and ϕ_5. (c) Pulse scheme of the HCACO–CBHB experiment. Prior to low-power decoupling (2.3 kHz field), a high-power $90^\circ_x 90^\circ_{\phi 10}$ pulse is applied (*18*). All details are identical to those of the HCACO–COSY experiment with the exception that the phase cycle used is $\phi_1 = 4(x)$, $4(-x)$; $\phi_2 = x, -x$; $\phi_3 = 8(x)$, $8(-x)$; $\phi_4 = 2(x)$, $2(-x)$; $\phi_5 = 16(x)$, $16(-x)$; $\phi_6 = 16(x)$, $16(-x)$; $\phi_7 = 8(x)$, $8(-x)$; $\phi_8 = x$; $\phi_9 = 4(x)$, $4(-x)$; $\phi_{10} = 4(x)$, $4(-x)$; Rec = x, $2(-x)$, x, $-x$, $2(x)$, $-x$. Quadrature in t_1 and t_2 is obtained using the States–TPPI method (*19*), incrementing the phases ϕ_2 and ϕ_8. In the present implementation of this experiment and the HCACO–COSY experiment, a delay equal to the duration of the C′ 180° pulse is inserted between the $C\alpha/\beta$ pulses ϕ_5 and ϕ_6 (HCACO–CBHB) or ϕ_8 and ϕ_9 (HCACO–COSY) in order to compensate for Cα chemical-shift evolution during application of the C′ 180° pulse (between f and g). Alternatively, an additional C′ 180° pulse can be inserted immediately before application of the pulses of phase ϕ_6 (HCACO–CBHB) or ϕ_9 (HCACO–COSY) to negate the phase error caused by the Bloch–Siegert shift (*21*) present during the first C′ 180° pulse and increase the sensitivity of the experiments.

Note that during the interval between points f and g, Cα magnetization dephases with respect to the attached Cβ spin as it rephases with respect to the C′ spin. Refocusing of the ^{13}C–^{13}C coupling and simultaneous dephasing due to the ^{1}H–^{13}C coupling occur during $2\tau_f$ so that at time h,

$$\rho_h = AS'_yI'_z\sin(2\pi J_{SS'}\tau_f)\prod_{K\neq S}\cos(2\pi J_{S'K}\tau_f)\cos(\omega_{S'}t_2), \quad [7]$$

where $J_{S'K}$ denotes the scalar coupling constant between spin S′ (Cβ) and a carbon K ($K \neq S$), $\omega_{S'}$ is the Larmor frequency of spin S′, the effects of multiple-bond ^{13}C–^{15}N couplings are neglected, and A is given by (*15*)

$$\begin{aligned} A &= \sin(2\pi J_{I'S'}\tau_e), && \text{for methines,}\\ A &= \sin(2\pi J_{I'S'}\tau_e)\cos(2\pi J_{I'S'}\tau_e), && \text{for methylenes,}\\ A &= 0.25\{\sin(2\pi J_{I'S'}\tau_e) + \sin(6\pi J_{I'S'}\tau_e)\}, && \text{for methyls.} \end{aligned} \quad [8]$$

The number of pulses is minimized by concatenation in a manner described previously (*16*). Finally, immediately before acquisition, the magnetization is given by

$$\rho = A\cos(\omega_{C'}t_1)\cos(\omega_{S'}t_2)\sin(2\pi J_{IS}\tau_a)\sin(2\pi J_{I'S'}\tau_a)\sin(2\pi J_{SC'}\tau_b)\cos(2\pi J_{SS'}\tau_b)$$
$$\times \sin(2\pi J_{SC'}\tau_c)\sin(2\pi J_{SS'}\tau_d)\sin(2\pi J_{SS'}\tau_f)\prod\cos(2\pi J_{S'K}\tau_f), \quad [9]$$

where all the previously omitted trigonometric factors have been included. Fourier transformation of the data yields peaks at coordinates ($\omega_{C'}$, $\omega_{S'}$, $\omega_{I'}$). In addition, peaks are found at coordinates ($\omega_{C'}$, ω_S, ω_I) since not all magnetization is transferred from Cα to Cβ during the COSY transfer. Thus, in addition to providing the Hβ and Cβ coordinates separated by the C′ chemical shift, this experiment also yields (C′, Cα, Hα) correlations in an analogous manner to the HCACO experiment (*9*).

Equation [9] indicates that carbonyl editing of side-chain COSY connectivities results in a sensitivity loss of a factor of 2–2.5 relative to that of the HCCH–COSY experiment for application to proteins the size of calmodulin. This sensitivity loss is kept at a minimum, in large part, due to the simultaneous refocusing and defocusing of scalar coupling interactions that occur during the course of the sequences. For example, in both the HCACO–COSY and the HCACO–CBHB experiments, Cα magnetization is refocused with respect to C′ spins as it dephases with respect to Cβ spins prior to COSY transfer of magnetization to the Cβ carbon. Unfortunately, the sensitivity of the HCACO–TOCSY experiment is reduced further since this experiment requires that Cα magnetization be refocused with respect to the coupled carbonyl spin prior to allowing the transfer of magnetization to side-chain carbons to occur via the TOCSY portion of the sequence. Nevertheless, as we shall illustrate below, the sensitivity of each of the experiments is sufficiently good for application to proteins at least as large as calmodulin.

The sequences described are illustrated on a 1.5 m*M* sample of ^{15}N, ^{13}C-labeled calmodulin from *Xenopus laevis,* complexed with 4 *M* equivalents of calcium, 0.1 *M* KCl, p*D* = 6.3, and dissolved in 0.5 ml D_2O. Experiments were performed on a Varian UNITY-500 spectrometer at 37°C. The size of each of the acquired data matrices for the HCACO–TOCSY and the HCACO–COSY experiments was 64 × 32 × 512 (Hα, C′, H$\alpha/\beta/\gamma\cdots$), where all numbers correspond to complex points and the acquisition

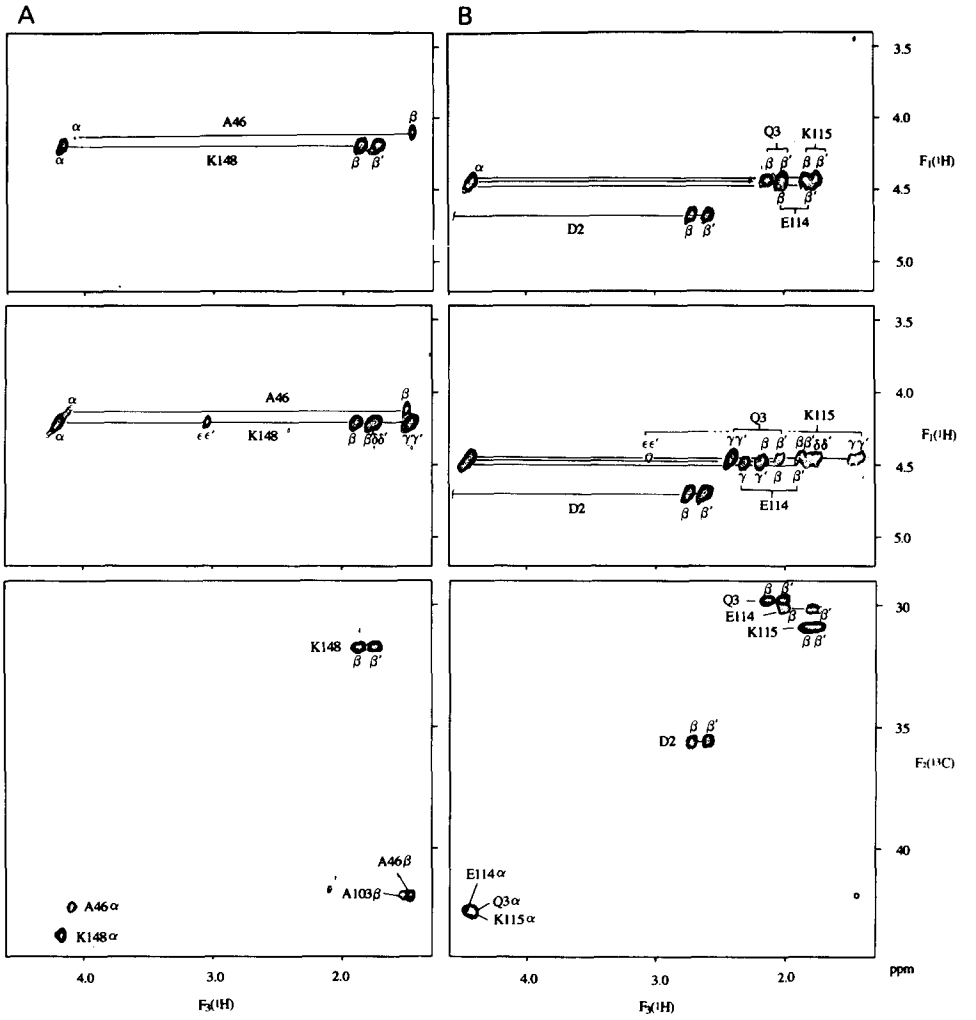

FIG. 2. Sections of slices from the HCACO-COSY (top) and HCACO-TOCSY (middle) (F_1/F_3) and HCACO-CBHB (bottom) (F_2/F_3) spectra of a 1.5 mM solution of *Xenopus laevis* calmodulin, recorded at 500 MHz, 37°C, pD = 6.8. Slices are at a carbonyl shift of 181.0 ppm (A) and 175.7 ppm (B). The HCACO-TOCSY and HCACO-COSY spectra were recorded as 64 × 32 × 512 complex data matrices. After zero-filling and Fourier transformation the matrix size of the absorptive part of the final 3D spectra was 128 × 64 × 1024. For the HCACO-CBHB experiment a data matrix of 48 × 32 × 512 was obtained. Linear prediction (*22*) was employed to extend the time-domain data in the t_2 dimension to 64 complex points. The absorptive part of the final 3D spectrum was 128 × 128 × 1024. Note that the (C′, Cβ, Hβ) cross peaks for A46 and A103 are folded. The data sets were processed using a combination of NMRi software (New Methods Research, Syracuse, New York) and software developed in house.

times were 32.0 ms (t_1), 21.3 ms (t_2), and 85.0 ms (t_3). In the case of the data set recorded with the HCACO-CBHB sequence, a matrix of 48 × 32 × 512 complex points (C′, Cα/β, Hα/β) was collected and the acquisition times were 32.0 ms (t_1), 7.1 ms (t_2), and 85.0 ms (t_3). A 32-step phase cycle was employed for each experiment with a delay of 0.8 s between scans, giving rise to a total measuring time of ~75 hours

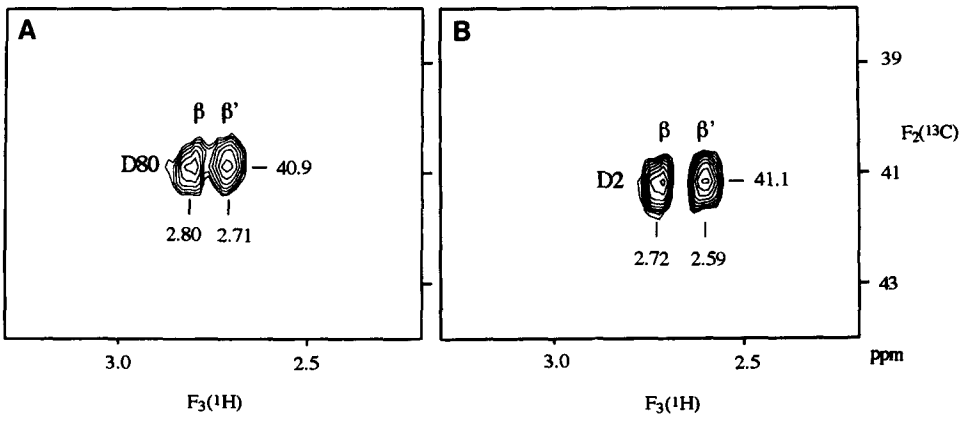

FIG. 3. Sections of the F_2/F_3 slices from the HCACO–CBHB spectrum of *Xenopus laevis* calmodulin at $F_1(^{13}C) = 176.8$ and 175.7 ppm. Although the Hα, Cα, and Cβ chemical shifts of residues D2 and D80 are within 0.05 and 0.40 ppm for the proton and carbon shifts, respectively, it is still possible to obtain accurate side-chain chemical shifts for these residues since their carbonyl chemical shifts are 1.1 ppm apart.

for the HCACO–TOCSY and HCACO–COSY data sets and ~55 hours for the HCACO–CBHB data set.

Figure 2 illustrates the quality of the data obtained from the various experiments discussed above. Slices taken at carbonyl chemical shifts of 181.0 ppm (Fig. 2A) and 175.7 ppm (Fig. 2B) are presented. Slices from the HCACO–COSY (HCACO–TOCSY) spectrum have the same appearance as slices from the HCCH–COSY (HCCH–TOCSY) spectrum, while slices from the HCACO–CBHB spectrum have a ^1H–^{13}C HMQC-type appearance. Note that in order to increase the resolution in the Cβ dimension of the HCACO–CBHB experiment, a spectral width of ±18 ppm was chosen in this dimension. This results in the folding of some of the cross peaks, such as those linking the (C', Cβ, Hβ) shifts of alanine residues. As with the HCCH–TOCSY experiment, the sensitivity of the HCACO–TOCSY experiment is sufficiently high that magnetization originating on the Cα carbon of lysine residues (K148 and K115 in Fig. 2) is relayed down the side chain to the Cϵ carbon. Figure 2B shows that despite the fact that the Hα and Cα chemical shifts of residues Q3, E114, and K115 overlap, it is straightforward to separate the Hβ resonances of the different residues in the slice from the HCACO–CBHB spectrum at 175.7 ppm.

Figure 3 shows portions of slices at carbonyl chemical shifts of 176.8 and 175.7 ppm. Although the differences in Hα, Cα, and Cβ chemical shifts for residues D2 and D80 are less than 0.05, 0.40, and 0.40 ppm, respectively, it is straightforward to distinguish the side-chain chemical shifts of each residue since their carbonyl chemical shifts are distinct. The accuracy of the determination of the Cβ and Hβ shifts from the HCCH–COSY and HCCH–TOCSY experiments is compromised as a result of the extensive overlap. In fact, based on analysis of the HCCH–COSY and HCCH–TOCSY spectra of calmodulin, the Hβ chemical shifts of D2 and D80 were previously thought to be degenerate (*8*). A close inspection of Fig. 3 yields more accurate Cβ and Hβ chemical shifts for both D2 and D80. In the case of calmodulin there are 15 pairs of residues that could be identified from the amino acids aspartic acid, glutamic

acid, asparagine, glutamine, and methionine, for which the differences in Hα, Cα, and Cβ chemical shifts are less than 0.05, 0.40, and 0.40 ppm, respectively (*8*). In over 30% of these cases the chemical shifts of the carbonyl resonances are sufficiently different to allow accurate determination of side-chain Hβ and Cβ shifts from the experiments described in this Communication. In cases where the carbonyl shifts of the residues are also degenerate, experiments which separate side-chain chemical shifts based on backbone ^{15}N shifts will prove extremely useful.

In this Communication we have presented a number of pulse schemes for the correlation of side-chain resonances in proteins, with separation achieved via the intra-residue carbonyl chemical shift. It is anticipated that these experiments will be most useful when used in concert with the existing HCCH–COSY and HCCH–TOCSY experiments. For residues having degenerate Hα and Cα chemical shifts, separation of peaks via the carbonyl shift may, in many cases, remove potential ambiguities in the assignment and aid in the development of an automated side-chain assignment protocol.

ACKNOWLEDGMENTS

We thank Dr. Claude Klee, Laboratory of Biochemistry, National Cancer Institute, National Institutes of Health, Bethesda, Maryland, for providing us with the *Xenopus laevis* calmodulin expression system, Dr. Dan Garrett, Laboratory of Chemical Physics, National Institutes of Diabetes and Digestive and Kidney Diseases, National Institutes of Health, Bethesda, Maryland, for providing a copy of his data analysis software, and Dr. Julie Forman-Kay, Hospital for Sick Children, Toronto, Ontario, for a critical evaluation of this manuscript. This work was supported by an operating grant from the Natural Sciences and Engineering Research Council of Canada to L.E.K.

REFERENCES

1. L. Braunschweiler and R. R. Ernst, *J. Magn. Reson.* **53,** 521 (1983).
2. D. G. Davis and A. Bax, *J. Am. Chem. Soc.* **107,** 2820 (1985).
3. W. P. Aue, E. Bartholdi, and R. R. Ernst, *J. Chem. Phys.* **64,** 2229 (1976).
4. L. E. Kay, M. Ikura, and A. Bax, *J. Am. Chem. Soc.* **112,** 888 (1990).
5. S. W. Fesik, H. L. Eaton, E. T. Olejniczak, E. R. P. Zuiderweg, L. P. McIntosh, and F. W. Dahlquist, *J. Am. Chem. Soc.* **112,** 886 (1990).
6. A. Bax, G. M. Clore, and A. M. Gronenborn, *J. Magn. Reson.* **88,** 425 (1990).
7. G. M. Clore, A. Bax, P. C. Driscoll, P. T. Wingfield, and A. M. Gronenborn, *Biochemistry* **29,** 8172 (1990).
8. M. Ikura, S. Spera, G. Barbato, L. E. Kay, M. Krinks, and A. Bax, *Biochemistry* **30,** 9216 (1991).
9. L. E. Kay, M. Ikura, R. Tschudin, and A. Bax, *J. Magn. Reson.* **89,** 496 (1990).
10. G. A. Morris and R. Freeman, *J. Am. Chem. Soc.* **101,** 760 (1979).
11. A. J. Shaka, J. Keeler, T. Frenkiel, and R. Freeman, *J. Magn. Reson.* **52,** 335 (1983).
12. A. Bax, M. Ikura, L. E. Kay, D. A. Torchia, and R. Tschudin, *J. Magn. Reson.* **86,** 304 (1990).
13. R. E. London, *J. Magn. Reson.* **86,** 410 (1990).
14. J. W. Peng, V. Thanabal, and G. Wagner, *J. Magn. Reson.* **95,** 421 (1991).
15. D. P. Burum and R. R. Ernst, *J. Magn. Reson.* **39,** 163 (1980).
16. L. E. Kay, M. Ikura, and A. Bax, *J. Magn. Reson.* **91,** 84 (1991).
17. A. J. Shaka, C. J. Lee, and A. Pines, *J. Magn. Reson.* **77,** 274 (1988).
18. A. Bax, G. M. Clore, P. C. Driscoll, A. M. Gronenborn, M. Ikura, and L. E. Kay, *J. Magn. Reson.* **87,** 620 (1990).
19. D. Marion, M. Ikura, R. Tschudin, and A. Bax, *J. Magn. Reson.* **85,** 393 (1989).
20. M. McCoy and L. Mueller, *J. Am. Chem. Soc.* **114,** 2108 (1992).
21. G. W. Vuister and A. Bax, *J. Magn. Reson.* **98,** 428 (1992).
22. H. Barkhuijsen, R. de Beer, W. M. M. J. Bovee, and D. Van Ormondt, *J. Magn. Reson.* **61,** 465 (1985).